Journal of Mechatronics, Electrical Power, and Vehicular Technology 8 (2017) 50–59

Journal of Mechatronics, Electrical Power, and Vehicular Technology

e-ISSN: 2088-6985
p-ISSN: 2087-3379

www.mevjournal.com

AFR and fuel cut-off modeling of LPG-fueled engine based on engine, transmission, and brake system using fuzzy logic controller (FLC)

Muji Setiyo*, Suroto Munahar

Department of Automotive Engineering, Universitas Muhammadiyah Magelang
Jl. Bambang Sugeng km.05 Mertoyudan Magelang 56172 Indonesia

Received 17 April 2017; received in revised form 2 June 2017; accepted 13 June 2017
Published online 31 July 2017

Abstract

During deceleration, continuous fuel flows into the engine not only causing over fuel consumption but also increasing exhausts emissions. Therefore, this paper presents a simulation of AFR and fuel cut-off modeling in the LPG-fueled vehicle using Fuzzy Logic Controller (FLC). The third generation of LPG kits (Liquid Phase Injection, LPI) was chosen due to its technological equivalency to EFI gasoline engine and promising to be developed. Given that the fuel system control is complex and non-linear, FLC has been selected because of simple, easy to understand, and tolerant to improper data. Simulation results show that the AFR and fuel cut-off controller able to maintenance AFR at the stoichiometric range during normal operation and able to cut the fuel flow at deceleration time for saving fuel and reducing emissions.

©2017 Research Centre for Electrical Power and Mechatronics - Indonesian Institute of Sciences. This is an open access article under the CC BY-NC-SA license (https://creativecommons.org/licenses/by-nc-sa/4.0/).

Keywords: LPG-fueled engine; deceleration; FLC; AFR; fuel cut-off

I. Introduction

Over the last decade, declining air quality, especially in urban areas has become a serious concern since it has direct impacts on human health. The transportation sector becomes a major contributor to increased air pollutant, emissions, and global greenhouse gas [1]. Now, most countries have implemented a policy of fuel economy standards for vehicles as an effective way to reduce oil consumption, carbon emissions, and air pollution. The internal combustion engine technology is also evolving in that direction [2, 3, 4, 5].

The use of LPG as an alternative fuel is also a trend in some countries as a medium-term solution, which until 2016, reportedly there are over 26 million LPG vehicles in use around the world and over 74,000 refueling sites [6]. Therefore, this paper presents a simulation of AFR controller and fuel cut-off during deceleration in the LPG-fueled engine as an effort to reduce fuel consumption and emissions.

Currently, the effort to reduce exhaust emissions from the automotive sector to improve urban air quality and public health is stronger than ever before [1, 2]. In the urban areas, particulate matter (PM) of the internal combustion engine has also become a concern [3, 4, 5]. Especially in the Spark Ignition (SI) engine, reducing fuel consumption and CO_2 are also a concern in the present.

In the last decades, the alternative automotive propulsion technologies such as fuel cells vehicles and electric vehicles have been commercialized as the green vehicles. However, fuel cell and electric vehicles will be facing the limited of mileage and high total cost of ownership [7]. Developing of bio-fuel as the alternative fuel will also be constrained by the availability of land for production [8, 9]. As a result, LPG will be a choice for at least two decades in the future as long as the price competes with gasoline [8]. On the other hand, fuel consumption and exhaust emissions from motor vehicles will be regulated more strictly [10].

Combustion with a lean mixture that is controlled by Engine Management Systems (EMS) becomes the trend development of today's LPG Engine [11]. In Indonesia, the implementation of low-emissions vehicles has become a Government program through

* Corresponding Author. Tel: +62 823 3062 3257
E-mail address: setiyo.muji@ummgl.ac.id

doi: https://dx.doi.org/10.14203/j.mev.2017.v8.50-59
2088-6985 / 2087-3379 ©2017 Research Centre for Electrical Power and Mechatronics - Indonesian Institute of Sciences (RCEPM LIPI).
This is an open access article under the CC BY-NC-SA license (https://creativecommons.org/licenses/by-nc-sa/4.0/).
Accreditation Number: (LIPI) 633/AU/P2MI-LIPI/03/2015 and (RISTEKDIKTI) 1/E/KPT/2015.

low-cost green car and low carbon emission program [12]. Initially, the Air to Fuel Ratio (AFR) entering the LPG engine was regulated only by converter and mixer or simple electronic control [13]. The stoichiometric mixture is obtained only at partial conditions. Now, the Liquid Phase Injection (LPI) of LPG-fueled engines has been supported by mechatronic systems with sensors, actuators, and control system (Figure 1).

Several treatments have also been made to improve performance, fuel economy, and emissions [14, 15]. AFR settings were intended to produce complete combustion throughout the engine load [16, 17]. In fact, the need for engine power is more than the fulfillment of low emissions. For example, tests performed by Massi and Gobbato, FIAT 838 A-1.000 engine describe the actual AFR is lower than stoichiometric AFR (15.7) for the most of the engine load, from 1000 rpm to 7000 rpm [18]. In the other case, there is significant variation in vehicle emissions during acceleration, deceleration, and cruising [19, 20].

The principle of LPI is the same as the gasoline EFI engine. Liquid LPG is supplied from the tank to the fuel rail and then injected into the intake manifold. LPG evaporation occurs entirely in the intake manifold [6]. The LPI system has the potential to achieve fuel savings, produce better power, and lower emissions than the VPI system. Subsequently, the main problem of AFR control is to solve the non-linear problem [22].

Nowadays, the look-up tables combining with the proportional and integral feedback controller is widely used for AFR control method because of its simple structure and robustness. However, this method is inefficient due to many engine variants and components [23]. The development of control technology also shows significant progress. Non-linear model predictive control (NMPC) has been attempted for SI engines to obtain the desired AFR in SI engine [24, 25, 26]. Studies conducted by Wang shows that the good control performance was obtained by adaptive radial basis function (RBF) model based NMPC method for AFR control [27].

Generally, AFR is controlled largely only by engine sensors. Meanwhile, the need for proper fuel in vehicles is not only influenced by the engine behavior but also influenced by the behavior of vehicles, such as braking condition and gear position. It is known that a car consists of a complex system with power flow as shown in Figure 2.

During acceleration, the engine drives the wheels so that the engine speed and vehicle speed are increased in accordance with the throttle valve opening. Conversely, the vehicle inertia makes the engine speed higher than the proportion of throttle valve opening during deceleration. Therefore, a possible method for controlling AFR is by using Fuzzy Logic Control (FLC) [22]. FLC was chosen by many researchers because it has relatively good system stability, able to resolve the black box problem, and can be applied on a Multi Input Multi Output (MIMO) [28, 29].

FLC has been widely applied to car engine control as AFR control, emissions, and torque [31, 32, 33]. However, the application for AFR control is the most popular researched. Most of the FLC applications on SI engines are to limit AFR in narrow bands around stoichiometric values to meet the limits imposed on automotive emissions with constraints from engine systems only. It consists of three sub-models that describe the dynamics of the intake manifold (including airflow, pressure, and air temperature), crankshaft speed, and fuel injection [33, 34].

AFR control based on the braking system was conducted by Triwiyatno *et al.* [35] that is quite promising to reduce fuel consumption. AFR control with additional external control of the engine is very likely to be developed. In addition to the brake system, another system that may be involved is the transmission system. In fact, wasted fuel is influenced by faulty transmission gear position. The combination of the engine, brake, and transmission systems as a controlling factor of AFR are particularly important, considering the vehicle often operates in downhill roads, highways, urban cycle, or in congestion [36, 37, 38].

In the previous study [39], AFR modeling on EFI engines based on engine dynamics, transmission, and vehicle dynamics also has been done without considering the dynamics of braking. As a result, the controller is unable to perform a fuel cut-off during vehicle deceleration below 80 mph.

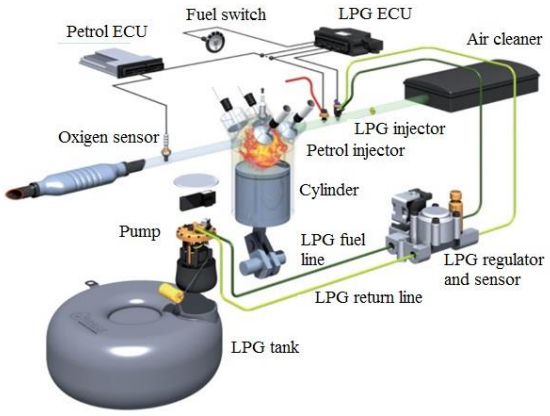

Figure 1. Liquid Phase Injection of LPG fuel systems [21]

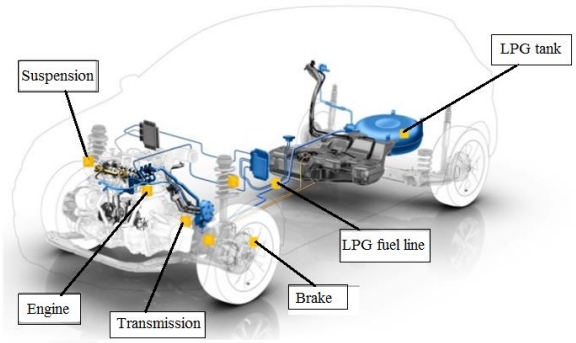

Figure 2. LPG-fueled vehicle propulsion and power train systems [30]

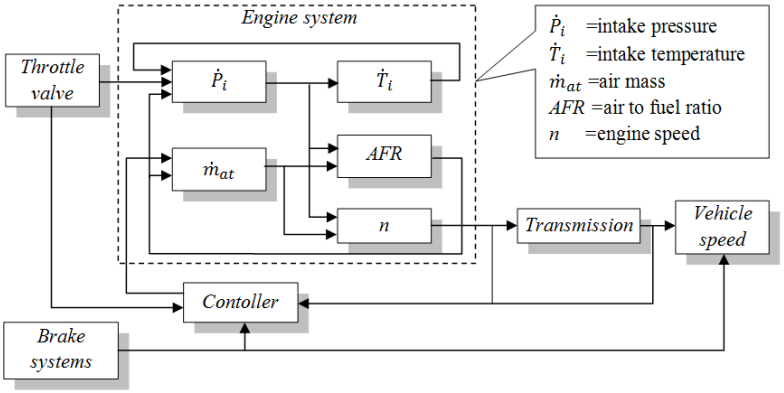

Figure 3. Block diagram of vehicle modeling for AFR controlling

Therefore, this paper presents the AFR modeling of LPI engine based on engine, brake, and transmission system using FLC to improve fuel efficiency. More specifically, in addition to controlling AFR, this study proposes a fuel cut-off method during the vehicle deceleration. By keeping the AFR in the stoichiometric range and making the fuel cut-off during deceleration that able to reduce emissions. The vehicle used in this study is Toyota 5A-FE which has been modified to LPG fuel systems.

II. Modelling

In this study, the throttle valve serves as the primary input to control engine speed. Subsequently, the engine rotation is distributed to the wheels of the vehicle through the gear box (transmission). The opening of the throttle valve increases engine speed which indicates vehicle acceleration. The vehicle deceleration occurs because of two conditions, braking or throttles valve closure without braking. The brake system not only serves to slow down the vehicle but also to control the fuel. So that the fuel control system has several inputs including vehicle speed, engine speed, throttle valve position and brake systems. Meanwhile, gear box provides the transmission ratio to change the vehicle speed. The Block diagram of vehicle modeling is presented in Figure 3.

A. Model of engine dynamics

Based on Figure 3, the opening of the throttle valve causes air to enter the intake chamber and then the engine cylinder through the engine valves. In this case, the mass of air entering the intake manifold is affected by pressure and temperature.

Without involving the EGR, formulation for intake pressure, intake temperature, and air mass that goes into the engine is presented in Equation (1), (2), (3), and (4), respectively.

$$\dot{P}_i = \frac{kR}{V_i}\left(-\dot{m}_{ap} + \dot{m}_{at}T_a\right) \quad (1)$$

$$\dot{T}i = \frac{RT_i}{P_iV_i}\left[-\dot{m}_{ap}(k-1)T_i + \dot{m}_{at}(kT_a - T_i)\right] \quad (2)$$

$$\dot{m}_{ap}\left(U, \dot{P}_i\right) = \dot{m}_{at1}\frac{Pa}{\sqrt{Ta}}\beta_1(U)\beta_2(P_r) + \dot{m}_{at0} \quad (3)$$

$$\dot{m}_{at}\left(U, \dot{P}_i\right) = \frac{V_d}{120RTi}(\eta_i.P_i)n \quad (4)$$

where $\dot{P}_i$ is the intake manifold pressure (bar). k is ratio of the specific heats (1.4 for air) and R is the constant of ideal gas (287 x 10^{-5}). V_i is the intake manifold volume in (m^3). $\dot{m}_{ap}$ and $\dot{m}_{at}$ are the air mass flow into intake port and air mass flow pass throttle plate (kg/s). T_a and T_i are the ambient temperature and intake air temperature (K). $\beta_1(U)$ is the throttle valve position and $\beta_1(P_r)$ is intake manifold pressure ratio [27]. V_d is engine displacement (m^3) and η_i is volumetric efficiency. Finally, n is the engine speed (rpm) and 120 is correction factor for four stroke SI engine.

The dynamics of the fuel injection also has been observed by Hendricks *et al.* [40] and Wang *et al.* [27]. The formulation of fuel dynamics is presented in Equation (5), (6), (7) and (8) as follows.

$$\dot{m}_{ff} = \frac{1}{\tau_f}(-\dot{m}_{ff} + X_f\dot{m}_{fi}) \quad (5)$$

$$\dot{m}_{fv} = (1\text{-}X_f)\dot{m}_{fi} \quad (6)$$

$$\dot{m}_f = \dot{m}_{fv}+\dot{m}_{ff} \quad (7)$$

$$X_f(P_i, n) = -0.27P_i - 0.055n + 0.68 \quad (8)$$

where, $\dot{m}_{ff}$, $\dot{m}_{fi}$, $\dot{m}_{fv}$, and $\dot{m}_f$ are the fuel film mass flow, injected fuel mass flow, fuel vapor mass flow, and engine port fuel mass flow (g/s), respectively. τ_f is the constant time of fuel evaporation and X_f is proportion of fuel. Meanwhile, τ_f is a function of the engine speed (n) and intake manifold pressure (P_i) with a formulation as in Equation (9). Then, AFR calculation is obtained from air mass flow into intake port $(\dot{m}_{ap})$ compared with the engine port fuel mass flow $(\dot{m}_f)$ (Equation 10).

$$\tau_f(P_i, n) = 1.35(-0.672n + 1.68)(P_i - 0.825)^2 + (0.06n + 0.15) + 0.56 \quad (9)$$

$$AFR = \frac{\dot{m}_{ap}}{\dot{m}_f} \quad (10)$$

The crankshaft speed dynamics($\dot{n}$) is presented in Equation (11). Intake manifold pressure (P_i), pumping power(P_p) and crankshaft speed have a relation to the friction power (P_f) and load power (P_b). Thus, stoichiometric AFR $(\lambda = 1)$, crankshaft speed (n), and the intake manifold pressure to be a factor of

indicated efficiency(η_i). $H_u$is fuel lower heating value (kJ/kg).

$$\dot{n} = \frac{1}{ln}(P_f(P_i, n) + P_p(P_i, n) + P_b(n) + \frac{1}{ln} H_u \eta_i(P_i, n, \lambda)\dot{m}_f(t - \Delta\tau_d) \quad (11)$$

The delay in the fuel injection system has been observed by Manzie *et al.* [41], which include injection systems, engine cycle, and exhaust valve expulsion. Injection delay model is presented in Equation (12) as follow.

$$\tau_d = 0.045 + \frac{10\pi}{n} \quad (12)$$

where, τ_d time delay of fuel injection system and 0.045 is propagation delay [17].

B. Model of drive train dynamics

In this study, the drive train is divided into two sub-systems (i.e. clutch and transmission). Clutch presented the mechanisms for connecting and disconnecting the engine speed to the transmission. The clutch system is presented in Equation (13). *K* is the capacity factor, N_{in} and N_e is the input transmission speed and engine speed in rpm, respectively. *f2/f3* is transmission ratio (gear). The torque ratio (RTQ) is formulated in Equation (14).

$$\mathrm{K} = \mathrm{f2}\frac{\mathrm{N_{in}}}{\mathrm{N_e}} \quad (13)$$

$$\mathrm{RTQ} = \mathrm{f3}\frac{\mathrm{N_{in}}}{\mathrm{N_e}} \quad (14)$$

Transmission ratio (R_{TR}) is obtained from the transmission gear ratio. T_{in} and T_{out} are the input and output torque of transmissin, respectively. N_{in} and N_{out} as the input and output speed of transmission shaft.

$$R_{TR} = \frac{N_{in}}{N_{out}} \quad (15)$$

Furthermore, the transmission ratio$(R_{TR})$of the vehicle used in this study is presented in Table 1 as follows.

C. Vehicle dynamics

The vehicle's movement is not only influenced by the engine speed but also by the vehicle inertia (I_v) and vehicle load variations [42]. Vehicle inertia is also affected by wheel speed (N_w) in rpm, final drive ratio (R_{fd}), load torque (T_{load}), and output transmission torque (T_{out}) as shown in Equation (16).

$$I_v . N_w = R_{fd} . (T_{out} - T_{load}) \quad (16)$$

A form of the vehicle body affects the speed of vehicles because of barriers surrounding air. Finally, road conditions also resulted in the brake operation.

$$T_{load} = sgn(mph)(R_{load0} + R_{load2} mph^2 + T_{brake}) \quad (17)$$

where, $R_{load0} R_{load2}$as the friction and coefficient drag, T_{brake} is the brake torque, and *mph* is the linier vehicle velocity.

Table 1.
Transmission ratio (R_{TR})

Gear Position	Transmission ratio (R_{TR})
1	3.55
2	1.91
3	1.31
4	0.97
5	0.82

D. Membership function

Fuzzy Logic Controller (FLC) requires the value of Membership Function (MF) as an input. MF is a curve that shows the points mapping of input data into membership values (degree of membership) which have the interval between 0 and 1. The MF curve is presented in Figure 4. Then, the fuzzy set decision is presented in Table 2 and Table 3. Fuel controller system approach is PID and fuzzy. Compensator formula controlled of PID is $P + I\frac{1}{2} + D\frac{N}{1+N\frac{1}{s}}$. The value proportional is 0.000003, Integral is 0.0027, and Derivative is 0.000005.

III. Result and discussion

A. Input condition

In this study, driving dynamic as driver behavior is presented in several sections. Throttle angle represents the throttle valve position in degree. Brake position represents the driver behavior when performing of vehicle deceleration. Braking signal generates by the hydraulic pressure sensor between 0 to 5 kg/cm². Hydraulic pressure above of 3 kg/cm² is considered as a braking condition to stop the vehicle and hydraulic pressure below of 3 kg/cm² is considered as the deceleration of the vehicle. Gear position represents the position of the transmission gear, from 1 to 4. The driving dynamic is divided into two modes. Braking mode as the driver presses the brake pedal and unbraking mode as the driver does not press the brake pedal. The relation between the driver behavior, controller, and vehicle dynamic is presented in Figure 5.

B. Deceleration at low speed

At the low speed, the engine is simulated for 10 seconds which represents an acceleration and deceleration. Referring to Figure 3 and Figure 5, the main input of the engine is a throttle valve position (0% means fully closed valve and 100% means fully opened valve).

The first period (0 seconds), the throttle valve is opened about 22%. The second period (from 0 to 10 second), the throttle valve is linear opened from 22% to 25%. The third period (exactly at 10 seconds), the throttle valve is closed from 25% to 19%. The third period is kept up to 30 seconds. Dynamics of throttle valve position and brake signal are presented in Figure 6.

It is known that when the throttle valve is opened, the air and fuel are sucked into the cylinder, and then combustion pressure will generate an engine speed.

The throttle valve is opened from 22% to 30% increasing the engine speed from 1000 rpm to 3200 rpm and increasing the vehicle speed from 0 mph to 82 mph.

In the time the throttle is closed abruptly (10 seconds), engine speed decreases to 2000 rpm (Figure 7a). However, the vehicle still cruised at high speed. The decrease in vehicle speed is not the same as a decrease in engine speed. Noting the equation (1) to (12) was processed by FLC, the results of engine speed and vehicle speed (with throttle valve position according to Figure 6) are presented in Figure 7. Without AFR controller, the fuel flowing into the cylinder is not required. Therefore, the effect of the controller to AFR is presented in Figure 8. In Figure 8a, there is an area where AFR is not detected. This

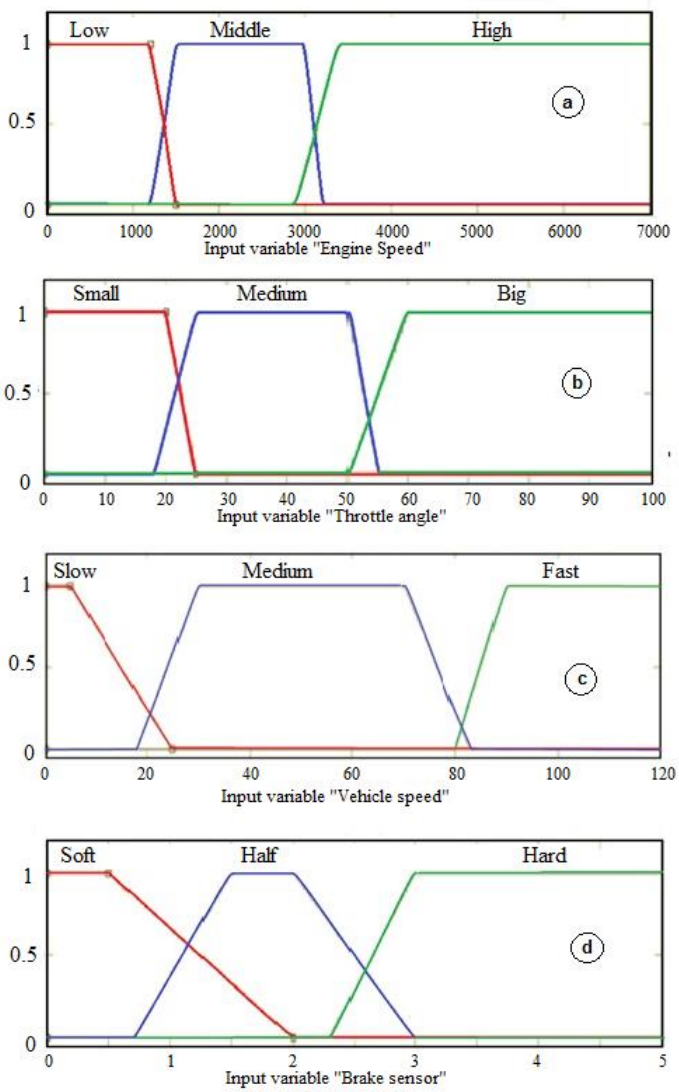

Figure 4. Membership function of (a) engine speed; (b) throttle angle; (c) vehicle speed; and (d) brake sensor

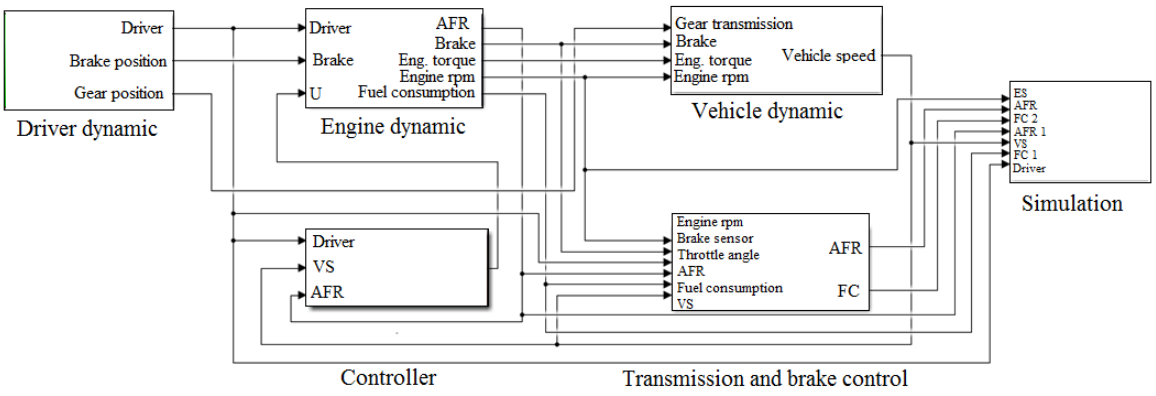

Figure 5. Vehicle modeling with transmission dan brake control system

Table 2.
Fuzzy set decision based on brake position “None” and "Soft

No	Engine Speed	Brake Position	Vehicle Speed	Throttle Angle	Decision
1	Low (0 to 1400 rpm)	None	Slow (0 to 25 mph)	Small (0 to 25 %)	off
2	Medium (1200 to 3200 rpm)	None	Slow (0 to 25 mph)	Small (0 to 25 %)	off
3	High (2800 to 7000 rpm)	None	Slow (0 to 25 mph)	Small (0 to 25 %)	off
4	Low (0 to 1400 rpm)	None	Medium (18 to 83 mph)	Small (0 to 25 %)	off
5	Medium (1200 to 3200 rpm)	None	Medium (18 to 83 mph)	Small (0 to 25 %)	off
6	High (2800 to 7000 rpm)	None	Medium (18 to 83 mph)	Small (0 to 25 %)	off
7	Low (0 to 1400 rpm)	None	Fast (80 to 120 mph)	Small (0 to 25 %)	off
8	Medium (1200 to 3200 rpm)	None	Fast (80 to 120 mph)	Small (0 to 25 %)	ON
9	High (2800 to 7000 rpm)	None	Fast (80 to 120 mph)	Small (0 to 25 %)	ON
10	Low (0 to 1400 rpm)	None	Slow (0 to 25 mph)	Medium (18 to 55 %)	off
11	Medium (1200 to 3200 rpm)	None	Slow (0 to 25 mph)	Medium (18 to 55 %)	off
12	High (2800 to 7000 rpm)	None	Slow (0 to 25 mph)	Medium (18 to 55 %)	off
13	Low (0 to 1400 rpm)	None	Medium (18 to 83 mph)	Medium (18 to 55 %)	off
14	Medium (1200 to 3200 rpm)	None	Medium (18 to 83 mph)	Medium (18 to 55 %)	off
15	High (2800 to 7000 rpm)	None	Medium (18 to 83 mph)	Medium (18 to 55 %)	off
16	Low (0 to 1400 rpm)	None	Fast (80 to 120 mph)	Medium (18 to 55 %)	off
17	Medium (1200 to 3200 rpm)	None	Fast (80 to 120 mph)	Medium (18 to 55 %)	off
18	High (2800 to 7000 rpm)	None	Fast (80 to 120 mph)	Medium (18 to 55 %)	off
19	Low (0 to 1400 rpm)	None	Slow (0 to 25 mph)	High (50 to 100 %)	off
20	Medium (1200 to 3200 rpm)	None	Slow (0 to 25 mph)	High (50 to 100 %)	off
21	High (2800 to 7000 rpm)	None	Slow (0 to 25 mph)	High (50 to 100 %)	off
22	Low (0 to 1400 rpm)	None	Medium (18 to 83 mph)	High (50 to 100 %)	off
23	Medium (1200 to 3200 rpm)	None	Medium (18 to 83 mph)	High (50 to 100 %)	off
24	High (2800 to 7000 rpm)	None	Medium (18 to 83 mph)	High (50 to 100 %)	off
25	Low (0 to 1400 rpm)	None	Fast (80 to 120 mph)	High (50 to 100 %)	off
26	Medium (1200 to 3200 rpm)	None	Fast (80 to 120 mph)	High (50 to 100 %)	off
27	High (2800 to 7000 rpm)	None	Fast (80 to 120 mph)	High (50 to 100 %)	off
28	Low (0 to 1400 rpm)	Soft (0 to 2 kg/cm²)	Slow (0 to 25 mph)	Small (0 to 25 %)	off
29	Medium (1200 to 3200 rpm)	Soft (0 to 2 kg/cm²)	Slow (0 to 25 mph)	Small (0 to 25 %)	off
30	High (2800 to 7000 rpm)	Soft (0 to 2 kg/cm²)	Slow (0 to 25 mph)	Small (0 to 25 %)	off
31	Low (0 to 1400 rpm)	Soft (0 to 2 kg/cm²)	Medium (18 to 83 mph)	Small (0 to 25 %)	off
32	Medium (1200 to 3200 rpm)	Soft (0 to 2 kg/cm²)	Medium (18 to 83 mph)	Small (0 to 25 %)	off
33	High (2800 to 7000 rpm)	Soft (0 to 2 kg/cm²)	Medium (18 to 83 mph)	Small (0 to 25 %)	off
34	Low (0 to 1400 rpm)	Soft (0 to 2 kg/cm²)	Fast (80 to 120 mph)	Small (0 to 25 %)	off
35	Medium (1200 to 3200 rpm)	Soft (0 to 2 kg/cm²)	Fast (80 to 120 mph)	Small (0 to 25 %)	ON
36	High (2800 to 7000 rpm)	Soft (0 to 2 kg/cm²)	Fast (80 to 120 mph)	Small (0 to 25 %)	ON
37	Low (0 to 1400 rpm)	Soft (0 to 2 kg/cm²)	Slow (0 to 25 mph)	Medium (18 to 55 %)	off
38	Medium (1200 to 3200 rpm)	Soft (0 to 2 kg/cm²)	Slow (0 to 25 mph)	Medium (18 to 55 %)	off
39	High (2800 to 7000 rpm)	Soft (0 to 2 kg/cm²)	Slow (0 to 25 mph)	Medium (18 to 55 %)	off
40	Low (0 to 1400 rpm)	Soft (0 to 2 kg/cm²)	Medium (18 to 83 mph)	Medium (18 to 55 %)	off
41	Low (0 to 1400 rpm)	Soft (0 to 2 kg/cm²)	Medium (18 to 83 mph)	Medium (18 to 55 %)	off
42	Medium (1200 to 3200 rpm)	Soft (0 to 2 kg/cm²)	Medium (18 to 83 mph)	Medium (18 to 55 %)	off
43	High (2800 to 7000 rpm)	Soft (0 to 2 kg/cm²)	Fast (80 to 120 mph)	Medium (18 to 55 %)	off
44	Low (0 to 1400 rpm)	Soft (0 to 2 kg/cm²)	Fast (80 to 120 mph)	Medium (18 to 55 %)	off
45	Medium (1200 to 3200 rpm)	Soft (0 to 2 kg/cm²)	Fast (80 to 120 mph)	Medium (18 to 55 %)	off
46	High (2800 to 7000 rpm)	Soft (0 to 2 kg/cm²)	Slow (0 to 25 mph)	High (50 to 100 %)	off
47	Low (0 to 1400 rpm)	Soft (0 to 2 kg/cm²)	Slow (0 to 25 mph)	High (50 to 100 %)	off
48	Medium (1200 to 3200 rpm)	Soft (0 to 2 kg/cm²)	Slow (0 to 25 mph)	High (50 to 100 %)	off

indicates that no fuel is injected into the engine, where the exhaust gas emissions are only air without combustion products. In Figure 8b, there is a fuel saving area, where this area is a fuel cut-off by the controller, i.e. no fuel flows to the engine.

C. Deceleration at high speed

As well as at low speeds, at high speed, the engine is simulated for 10 seconds which represents an acceleration and deceleration. Referring to Figure 3 and Figure 5, the main input of the engine is a throttle valve position. The first period (0 seconds), the throttle valve is opened 22%.

Table 3.
Fuzzy set decision based on brake position “Half” and “Hard”

No	Engine Speed	Brake Position	Vehicle Speed	Throttle Angle	Decision
49	High (2800 to 7000 rpm)	Half (0.7 to 3 kg/cm²)	Medium (18 to 83 mph)	High (50 to 100 %)	off
50	Low (0 to 1400 rpm)	Half (0.7 to 3 kg/cm²)	Medium (18 to 83 mph)	High (50 to 100 %)	off
51	Medium (1200 to 3200 rpm)	Half (0.7 to 3 kg/cm²)	Medium (18 to 83 mph)	High (50 to 100 %)	off
52	High (2800 to 7000 rpm)	Half (0.7 to 3 kg/cm²)	Fast (80 to 120 mph)	High (50 to 100 %)	off
53	Low (0 to 1400 rpm)	Half (0.7 to 3 kg/cm²)	Fast (80 to 120 mph)	High (50 to 100 %)	off
54	Medium (1200 to 3200 rpm)	Half (0.7 to 3 kg/cm²)	Fast (80 to 120 mph)	High (50 to 100 %)	off
55	High (2800 to 7000 rpm)	Half (0.7 to 3 kg/cm²)	Slow (0 to 25 mph)	Small (0 to 25 %)	off
56	Low (0 to 1400 rpm)	Half (0.7 to 3 kg/cm²)	Slow (0 to 25 mph)	Small (0 to 25 %)	ON
57	Medium (1200 to 3200 rpm)	Half (0.7 to 3 kg/cm²)	Slow (0 to 25 mph)	Small (0 to 25 %)	ON
58	High (2800 to 7000 rpm)	Half (0.7 to 3 kg/cm²)	Medium (18 to 83 mph)	Small (0 to 25 %)	off
59	Low (0 to 1400 rpm)	Half (0.7 to 3 kg/cm²)	Medium (18 to 83 mph)	Small (0 to 25 %)	off
60	Medium (1200 to 3200 rpm)	Half (0.7 to 3 kg/cm²)	Medium (18 to 83 mph)	Small (0 to 25 %)	off
61	High (2800 to 7000 rpm)	Half (0.7 to 3 kg/cm²)	Fast (80 to 120 mph)	Small (0 to 25 %)	off
62	Low (0 to 1400 rpm)	Half (0.7 to 3 kg/cm²)	Fast (80 to 120 mph)	Small (0 to 25 %)	off
63	Low (0 to 1400 rpm)	Half (0.7 to 3 kg/cm²)	Fast (80 to 120 mph)	Small (0 to 25 %)	off
64	Medium (1200 to 3200 rpm)	Half (0.7 to 3 kg/cm²)	Slow (0 to 25 mph)	Medium (18 to 55 %)	off
65	High (2800 to 7000 rpm)	Half (0.7 to 3 kg/cm²)	Slow (0 to 25 mph)	Medium (18 to 55 %)	off
66	Low (0 to 1400 rpm)	Half (0.7 to 3 kg/cm²)	Slow (0 to 25 mph)	Medium (18 to 55 %)	off
67	Medium (1200 to 3200 rpm)	Half (0.7 to 3 kg/cm²)	Medium (18 to 83 mph)	Medium (18 to 55 %)	off
68	High (2800 to 7000 rpm)	Half (0.7 to 3 kg/cm²)	Medium (18 to 83 mph)	Medium (18 to 55 %)	off
69	Low (0 to 1400 rpm)	Half (0.7 to 3 kg/cm²)	Medium (18 to 83 mph)	Medium (18 to 55 %)	off
70	Medium (1200 to 3200 rpm)	Half (0.7 to 3 kg/cm²)	Fast (80 to 120 mph)	Medium (18 to 55 %)	off
71	High (2800 to 7000 rpm)	Half (0.7 to 3 kg/cm²)	Fast (80 to 120 mph)	Medium (18 to 55 %)	off
72	Low (0 to 1400 rpm)	Half (0.7 to 3 kg/cm²)	Fast (80 to 120 mph)	Medium (18 to 55 %)	off
73	Medium (1200 to 3200 rpm)	Half (0.7 to 3 kg/cm²)	Slow (0 to 25 mph)	High (50 to 100 %)	off
74	High (2800 to 7000 rpm)	Half (0.7 to 3 kg/cm²)	Slow (0 to 25 mph)	High (50 to 100 %)	off
75	Low (0 to 1400 rpm)	Half (0.7 to 3 kg/cm²)	Slow (0 to 25 mph)	High (50 to 100 %)	off
76	Medium (1200 to 3200 rpm)	Hard (2.3 to 5 kg/cm²)	Medium (18 to 83 mph)	High (50 to 100 %)	off
77	High (2800 to 7000 rpm)	Hard (2.3 to 5 kg/cm²)	Medium (18 to 83 mph)	High (50 to 100 %)	off
78	Low (0 to 1400 rpm)	Hard (2.3 to 5 kg/cm²)	Medium (18 to 83 mph)	High (50 to 100 %)	off
79	Medium (1200 to 3200 rpm)	Hard (2.3 to 5 kg/cm²)	Fast (80 to 120 mph)	High (50 to 100 %)	off
80	High (2800 to 7000 rpm)	Hard (2.3 to 5 kg/cm²)	Fast (80 to 120 mph)	High (50 to 100 %)	off
81	Low (0 to 1400 rpm)	Hard (2.3 to 5 kg/cm²)	Fast (80 to 120 mph)	High (50 to 100 %)	off
82	Medium (1200 to 3200 rpm)	Hard (2.3 to 5 kg/cm²)	Slow (0 to 25 mph)	Small (0 to 25 %)	off
83	High (2800 to 7000 rpm)	Hard (2.3 to 5 kg/cm²)	Slow (0 to 25 mph)	Small (0 to 25 %)	off
84	Low (0 to 1400 rpm)	Hard (2.3 to 5 kg/cm²)	Slow (0 to 25 mph)	Small (0 to 25 %)	ON
85	Low (0 to 1400 rpm)	Hard (2.3 to 5 kg/cm²)	Medium (18 to 83 mph)	Small (0 to 25 %)	ON
86	Medium (1200 to 3200 rpm)	Hard (2.3 to 5 kg/cm²)	Medium (18 to 83 mph)	Small (0 to 25 %)	off
87	High (2800 to 7000 rpm)	Hard (2.3 to 5 kg/cm²)	Medium (18 to 83 mph)	Small (0 to 25 %)	off
88	Low (0 to 1400 rpm)	Hard (2.3 to 5 kg/cm²)	Fast (80 to 120 mph)	Small (0 to 25 %)	off
89	Medium (1200 to 3200 rpm)	Hard (2.3 to 5 kg/cm²)	Fast (80 to 120 mph)	Small (0 to 25 %)	off
90	High (2800 to 7000 rpm)	Hard (2.3 to 5 kg/cm²)	Fast (80 to 120 mph)	Small (0 to 25 %)	off
91	Low (0 to 1400 rpm)	Hard (2.3 to 5 kg/cm²)	Slow (0 to 25 mph)	Medium (18 to 55 %)	off
92	Medium (1200 to 3200 rpm)	Hard (2.3 to 5 kg/cm²)	Slow (0 to 25 mph)	Medium (18 to 55 %)	off
93	High (2800 to 7000 rpm)	Hard (2.3 to 5 kg/cm²)	Slow (0 to 25 mph)	Medium (18 to 55 %)	off
94	Low (0 to 1400 rpm)	Hard (2.3 to 5 kg/cm²)	Medium (18 to 83 mph)	Medium (18 to 55 %)	off
95	Medium (1200 to 3200 rpm)	Hard (2.3 to 5 kg/cm²)	Medium (18 to 83 mph)	Medium (18 to 55 %)	off
96	High (2800 to 7000 rpm)	Hard (2.3 to 5 kg/cm²)	Medium (18 to 83 mph)	Medium (18 to 55 %)	off
97	Low (0 to 1400 rpm)	Hard (2.3 to 5 kg/cm²)	Fast (80 to 120 mph)	Medium (18 to 55 %)	off
98	Medium (1200 to 3200 rpm)	Hard (2.3 to 5 kg/cm²)	Fast (80 to 120 mph)	Medium (18 to 55 %)	off
99	High (2800 to 7000 rpm)	Hard (2.3 to 5 kg/cm²)	Fast (80 to 120 mph)	Medium (18 to 55 %)	off
100	Low (0 to 1400 rpm)	Hard (2.3 to 5 kg/cm²)	Slow (0 to 25 mph)	High (50 to 100 %)	off
101	Medium (1200 to 3200 rpm)	Hard (2.3 to 5 kg/cm²)	Slow (0 to 25 mph)	High (50 to 100 %)	off
102	High (2800 to 7000 rpm)	Hard (2.3 to 5 kg/cm²)	Slow (0 to 25 mph)	High (50 to 100 %)	off

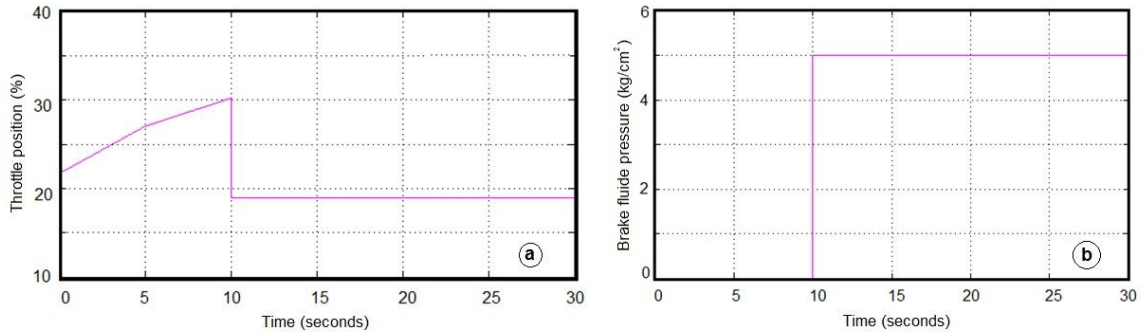

Figure 6. Simulation of (a) throttle valve position; and (b) brake signal from 0 to 30 seconds

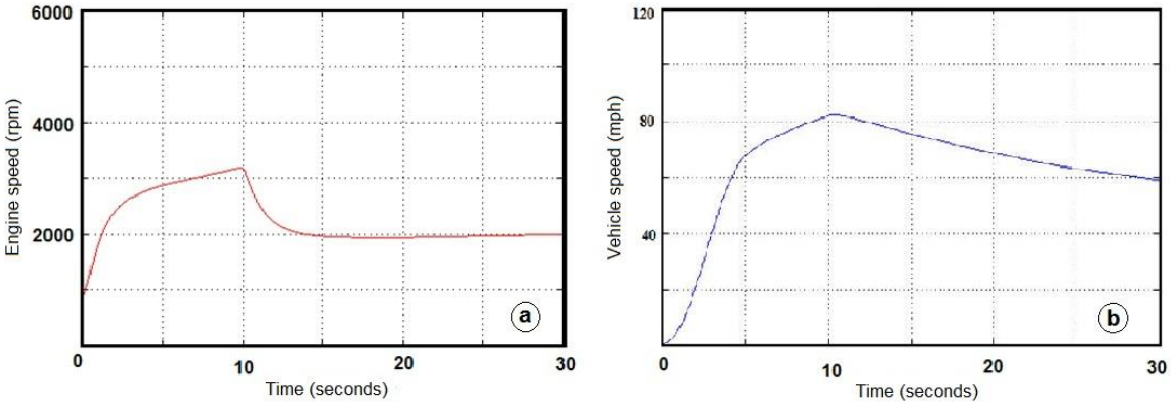

Figure 7. Engine speed (a) and vehicle speed (b) from 0 to 30 seconds based on throttle position and brake signal from Figure 5

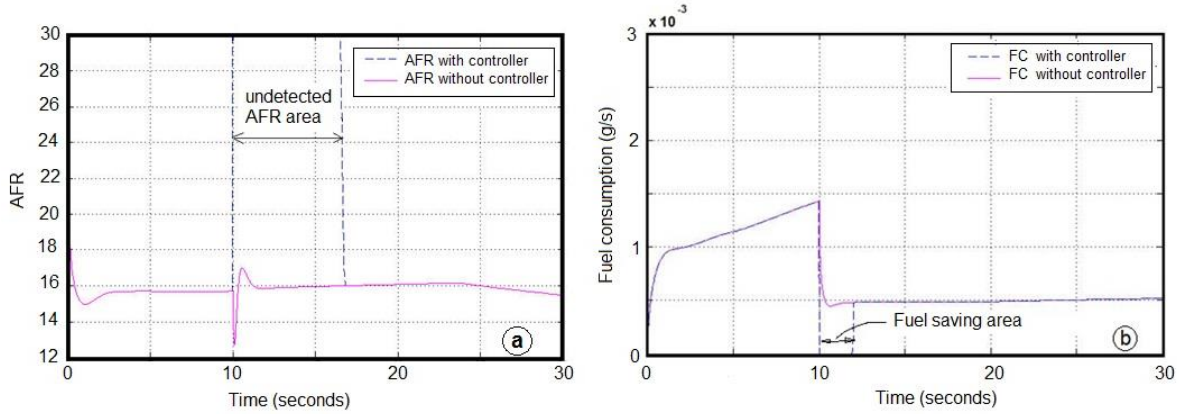

Figure 8. AFR (a) and fuel consumption (b) from 0 to 30 seconds based on throttle position and brake signal from Figure 6

The second period (from 0 to 10 second), the throttle valve is linear opened from 22% to 38%. The third period (exactly at 10 seconds), the throttle valve is closed from 30% to 19% respectively. The third period is kept up to 30 seconds. Dynamics of throttle valve angle is presented in Figure 9.

When the throttle valve is opened from 22 % to 38 %, the engine capable of operating up to 4200 rpm and vehicle speed reaches 110 mph. At the time of the gas pedal is released suddenly (10 seconds), the engine fell into 2000 rpm. However, this condition is not followed by a decrease in vehicle speed. The dynamics of the engine and vehicle speed are presented in Figure 10 and Figure 11, respectively.

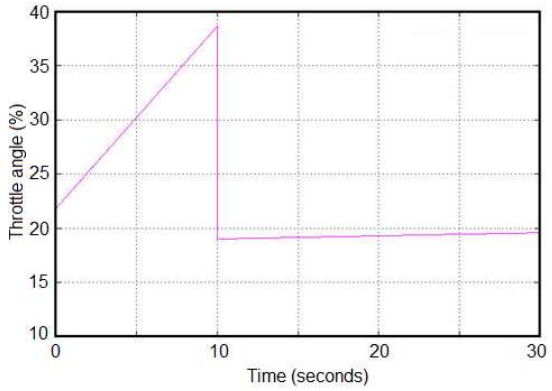

Figure 9. Simulation of throttle valve dynamics at high engine speed

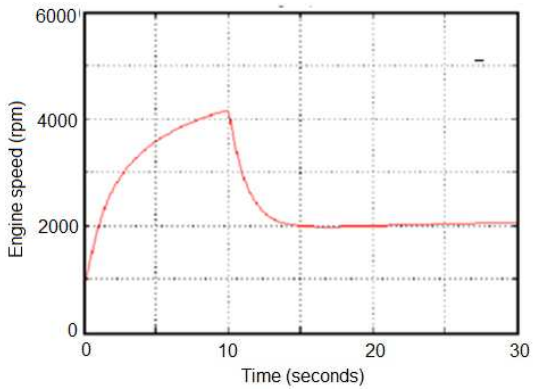

Figure 10. Engine speed based on throttle dynamics from Figure 9

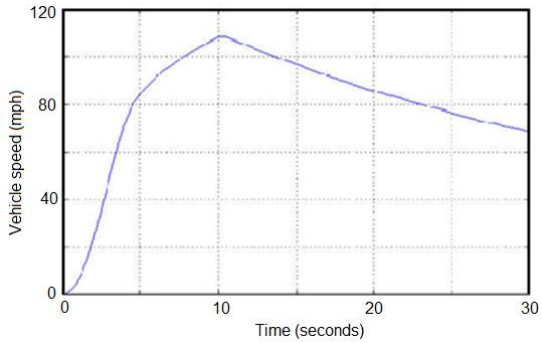

Figure 11.Vehicle speed based on throttle dynamics from Figure 8

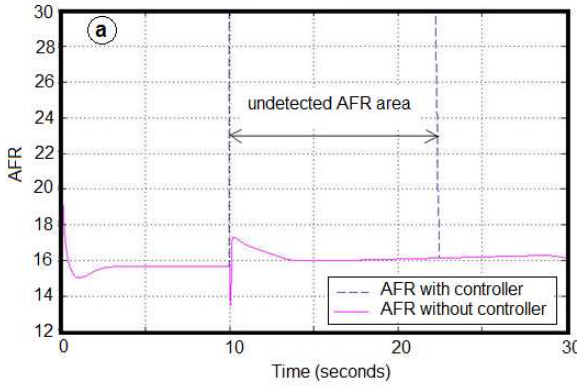

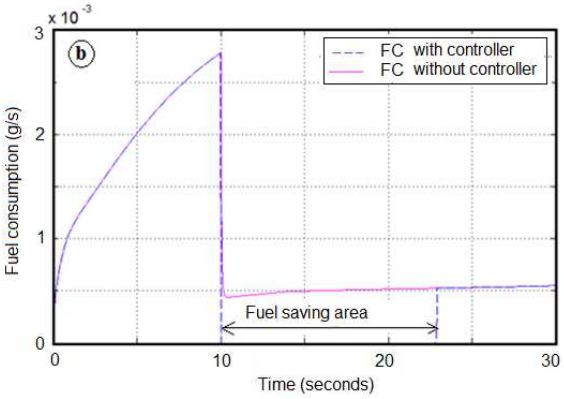

Figure 12. (a) AFR; and (b) fuel consumption from 0 to 30 seconds based at the time of deceleration from high speed

AFR dynamics generated during deceleration time is presented in Figure 12(a). Initially, AFR value shows at 15.6. At the time of throttle valve closed, AFR is illegible. This means the economizer works and no fuel injected into the engine. As a result, there is a fuel-cutting area for 13 seconds, showed in Figure 12(b). This shows significant fuel savings during vehicle deceleration, without interfere the vehicle performance during acceleration and cruising.

IV. Conclusion

A series of simulation results indicates that modeling FLC to AFR controlling cut-off fuel during deceleration on LPI-LPG fueled engine which is a non-linear condition can be applied at low speed and high speed condition. The throttle valve position, engine speed, transmission system, and brake operation were able to control the AFR and fuel flow into the engine in the desired condition. At the time of deceleration, AFR is not detected for several times, which means there is no fuel flow from fuel line into the engine. In conclusion, FLC is a promising to be applied on LPI-LPG fueled engine for fuel saving.

Acknowledgement

This research is fully supported by Automotive Laboratory and Research Division of Universitas Muhammadiyah Magelang. The researchers are grateful to both institutions.

References

[1] GFEI, “Improving Vehicle Fuel Economy in the ASEAN Region,” London, 2010.
[2] S. Karagiorgis *et al.*, “Control Challenges in Automotive Engine Management,” European *Journal of Control*, vol. 13, no. 2–3, pp. 92–104, Jan. 2007.
[3] S. T. Anderson *et al.*, “Automobile fuel economy standards: Impacts, efficiency, and alternatives,” *Review of Environmental Economics and Policy*, vol. 5, no. 1, pp. 89–108, 2011.
[4] K. Ravi and E. Porpatham, “Effect of piston geometry on performance and emission characteristics of an LPG fuelled lean burn SI engine at full throttle condition,” *Applied Thermal Engineering*, vol. 110, pp. 1051–1060, 2017.
[5] M. El-Faroug *et al.*, “Spark Ignition Engine Combustion, Performance and Emission Products from Hydrous Ethanol and Its Blends with Gasoline,” *Energies*, vol. 9, no. 12, p. 984, 2016.
[6] World LPG Association, “Autogas Incentive Policies, 2015 Update,” Neuilly-sur-Seine, 2015.
[7] M. Messagie *et al.*, “Environmental and financial evaluation of passenger vehicle technologies in Belgium,” *Sustainability (Switzerland)*, vol. 5, no. 12, pp. 5020–5033, 2013.
[8] M. Setiyo *et al.*, “Techno-economic analysis of liquid petroleum gas fueled vehicles as public transportation in Indonesia,” *International Journal of Energy Economics and Policy*, vol. 6, no. 3, pp. 495–500, 2016.
[9] IEA, “Biofuels for transport in 2050,” Paris, 2011.
[10] F. An *et al.*, “Global overview on fuel efficiency and motor vehicle emission standards: policy options and perspectives for international cooperation,” New York, 2011.
[11] World LPG Association, “Autogas Incentive Policies,” Neuilly-sur-Seine, 2016.
[12] Gaikindo, “Indonesia Automotive Industry Report on 2013 Auto Market,” in *The 20th APEC Automotive Dialogue*, 2014, no. April.

[13] M. Setiyo *et al.*, "Characteristics of 1500 cc LPG fueled engine at various of mixer venturi area applied on tesla A-100 LPG vaporizer," *Jurnal Teknologi*, vol. 78, no. 10, pp. 43–49, 2016.
[14] F. Hofmann, Converting *Vehicles to Propane Autogas Part 4: Troubleshooting Four Current Autogas Fuel Systems*. Washington, D.C, USA: Propane Education & Research Council, 2012.
[15] A. Kaleli *et al.*, "Controlling spark timing for consecutive cycles to reduce the cyclic variations of SI engines," *Applied Thermal Engineering*, vol. 87, pp. 624–632, 2015.
[16] C. Park *et al.*, "Combustion and Emission Characteristics According to the Fuel Injection Ratio of an Ultra-Lean LPG Direct Injection Engine," *Energies*, vol. 9, no. 11, p. 920, 2016.
[17] C. Manzie *et al.*, "Air Fuel Ratio Control In Liquefied Petroleum Gas Injected SI Engines," in *Triennial World Congress*, 2002.
[18] M. Masi and P. Gobbato, "Measure of the volumetric efficiency and evaporator device performance for a liquefied petroleum gas spark ignition engine," *Energy Conversion and Management*, vol. 60, pp. 18–27, 2012.
[19] J. Gallus *et al.*, "Impact of driving style and road grade on gaseous exhaust emissions of passenger vehicles measured by a Portable Emission Measurement System (PEMS)," *Transportation Research Part D: Transport and Environment*, vol. 52, no. 2, pp. 215–226, 2017.
[20] Y. Zhang et.*al*, "Evaluation of vehicle acceleration models for emission estimation at an intersection," *Transportation Research Part D: Transport and Environment*, vol. 18, no. 1, pp. 46–50, 2013.
[21] Gazeo, "Autogas system generations," *Global LPG & CNG Portal*, 2012. [Online]. Available: http://gazeo.com/automotive/technology/Autogas-system-generations,article,6486.html. [Accessed: 23-May-2017].
[22] B. A. Al-himyari *et al.*, "Review of Air-Fuel Ratio Prediction and Control Methods," *Asian Journal of Applied Sciences*, vol. 2, no. 4, pp. 471–478, 2014.
[23] Y. Shi *et al.*, "Air-fuel ratio prediction and NMPC for SI engines with modified Volterra model and RBF network," *Engineering Applications of Artificial Intelligence*, vol. 45, pp. 313–324, 2015.
[24] Y.-J. Zhai and D.-L. Yu, "Neural network model-based automotive engine air/fuel ratio control and robustness evaluation," *Engineering Applications of Artificial Intelligence*, vol. 22, no. 2, pp. 171–180, 2009.
[25] S. Wang and D. L. Yu, "Adaptive RBF network for parameter estimation and stable air–fuel ratio control," *Neural Networks*, vol. 21, no. 1, pp. 102–112, 2008.
[26] I. Arsie *et al.*, "A procedure to enhance identification of recurrent neural networks for simulating air–fuel ratio dynamics in SI engines," *Engineering Applications of Artificial Intelligence*, vol. 19, no. 1, pp. 65–77, 2006.
[27] S. W. Wang *et al.*, "Adaptive neural network model based predictive control for air-fuel ratio of SI engines," *Engineering Applications of Artificial Intelligence*, vol. 19, no. 2, pp. 189–200, 2006.
[28] T. M. Guerra *et al.*, "Conditions of output stabilization for nonlinear models in the Takagi-Sugeno's form," *Fuzzy Sets and Systems*, vol. 157, no. 9, pp. 1248–1259, 2006.
[29] M. Zhou *et al.*, "A review of vehicle fuel consumption models to evaluate eco-driving and eco-routing," *Transportation Research Part D: Transport and Environment*, vol. 49, pp. 203–218, 2016.
[30] C. G. Foster *et al.*, "Automobile," *Encyclopædia Britannica*. [Online]. Available: https://www.britannica.com/technology/automobile. [Accessed: 11-Dec-2016].
[31] Mohammad Al Zubi and Ayman M. Mansour, "Detection of Automotive Emissions Status using Fuzzy Inference System \n," *IOSR Journal of Mechanical and Civil Engineering (IOSR-JMCE)*, vol. 10, no. 4, pp. 17–23, 2013.
[32] A. Triwiyatno *et al.*, "Engine Torque Control of Spark Ignition Engine Using Robust Fuzzy Logic Control," *IACSIT International Journal of Engineering and Technology*, vol. 3, no. 4, pp. 352–358, 2011.
[33] M. J. Nekooei and J. Koto, "Hybrid Fuzzy Logic Controller in Matlab / Simulink for Controlling AFR of SI Engine," *International Journal of Environmental Research & Clean Energy*, vol. 5, no. 1, pp. 11–20, 2017.
[34] A. Ghaffari *et al.*, "Adaptive Fuzzy Control for Air-Fuel Ratio of Automobile Spark Ignition Engine," *Engineering and Technology*, pp. 284–292, 2008.
[35] A. Triwiyatno *et al.*, "Smart controller design of air to fuel ratio (AFR) and brake control system on gasoline engine," in *ICITACEE 2015 - 2nd International Conference on Information Technology, Computer, and Electrical Engineering*, 2016, pp. 233–238.
[36] K. Zhang *et al.*, "Vehicle emissions in congestion: Comparison of work zone, rush hour and free-flow conditions," *Atmospheric Environment*, vol. 45, no. 11, pp. 1929–1939, 2011.
[37] J. Edquist *et al.*, *Road* design *factors and their interactions with speed and speed limits - Report 298*. 2009.
[38] J. D. Clapp *et al.*, "The driving behavior survey: Scale construction and validation," *Journal of Anxiety Disorders*, vol. 25, no. 1, pp. 96–105, 2011.
[39] S. Munahar and M. Setiyo, "AFR Modeling of EFI Engine Based on Engine Dynamics, Vehicle Dynamics, and Transmission System," *Jurnal Teknik Mesin*, vol. 7, no. 1, pp. 21–29, 2017.
[40] E. Hendricks *et al.*, "A generic mean value engine model for spark ignition engines," in *Proceedings of the 41st Simulation Conference SIMS*, 2000.
[41] C. Manzie *et al.*, "Model predictive control of a fuel injection system with a radial basis function network observer," *Journal of Dynamic Systems, Measurement and Control, Transactions of the ASME*, vol. 124, no. 4, pp. 648–658, 2002.
[42] Mathworks, "Modeling an Automatic Transmission Controller," *Mathworks Documentation*. 2016.